

**Current Biology, Volume 29**

**Supplemental Information**

**Neuronal XBP-1 Activates Intestinal**

**Lysosomes to Improve Proteostasis in *C. elegans***

**Soudabeh Imanikia, Neşem P. Özbey, Christel Krueger, M. Olivia Casanueva, and Rebecca C. Taylor**

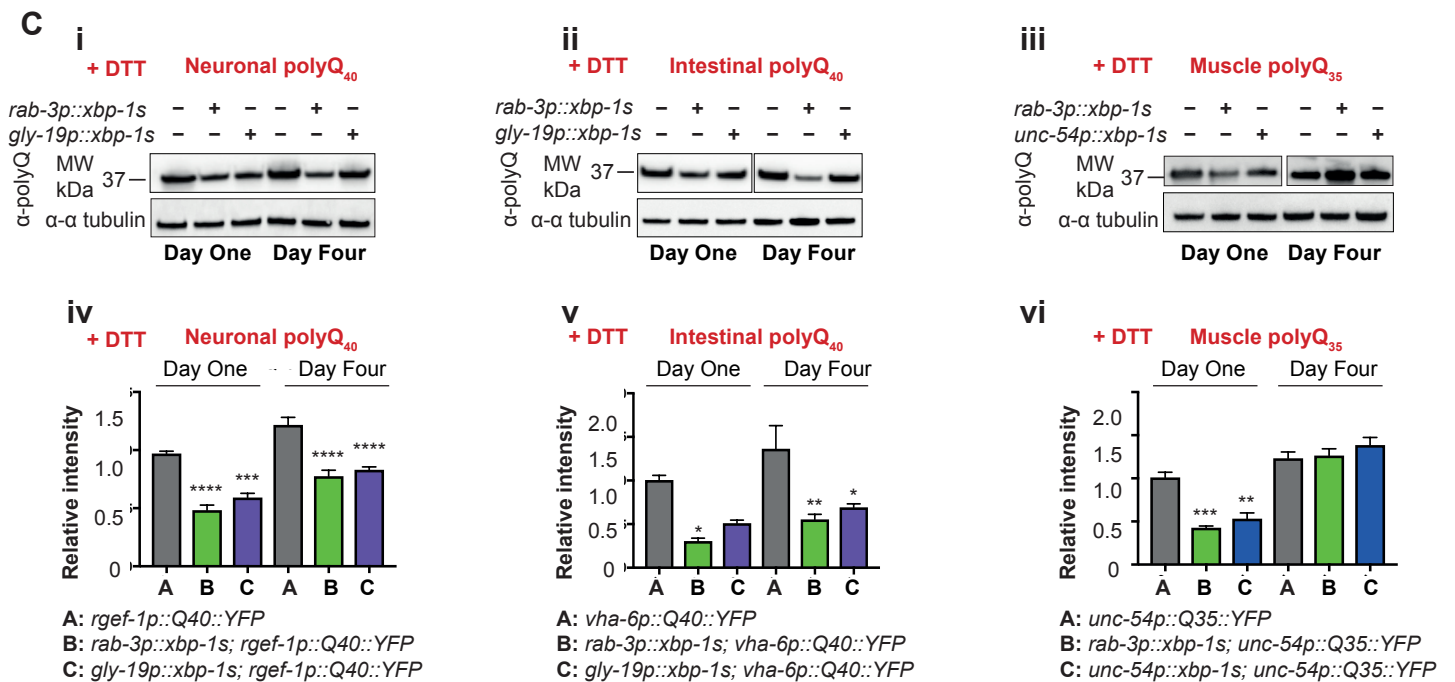
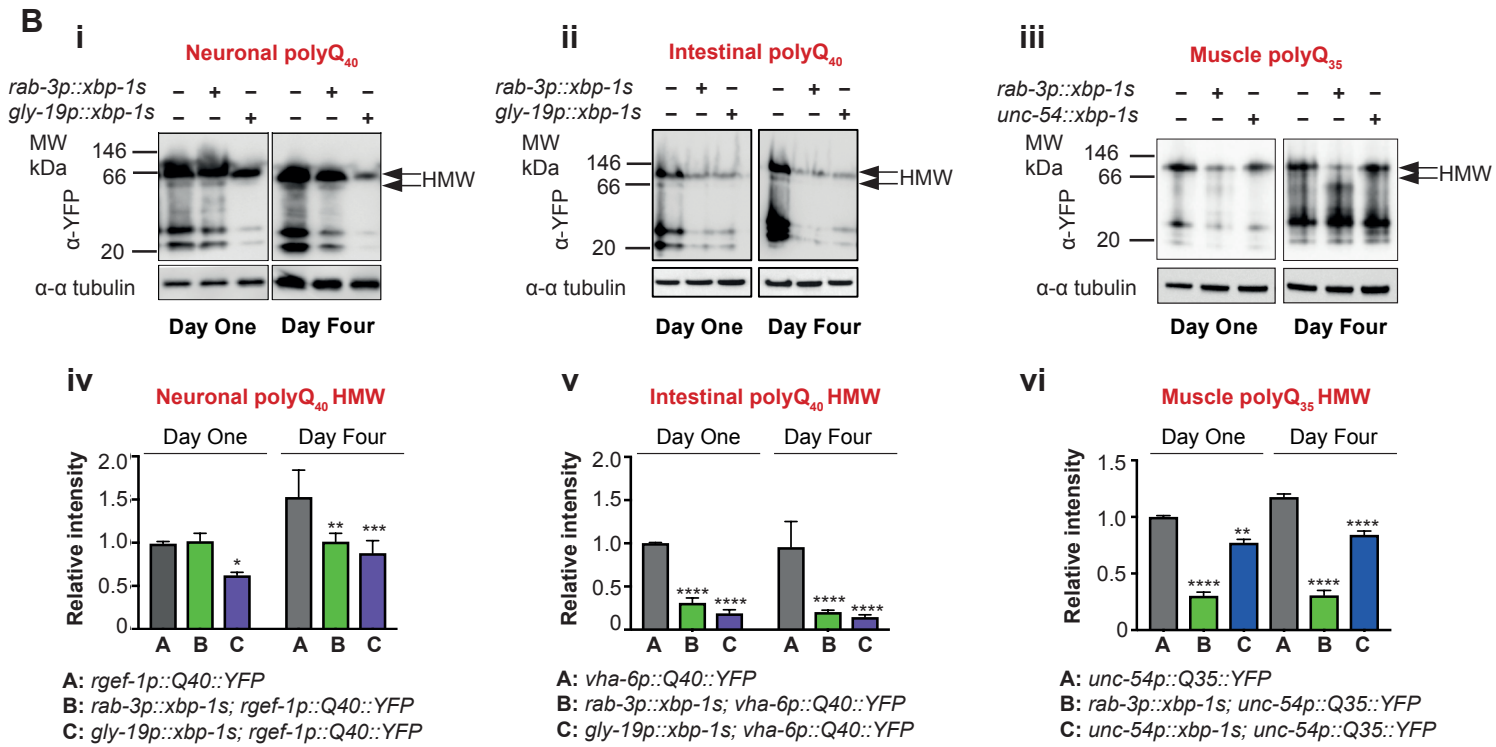
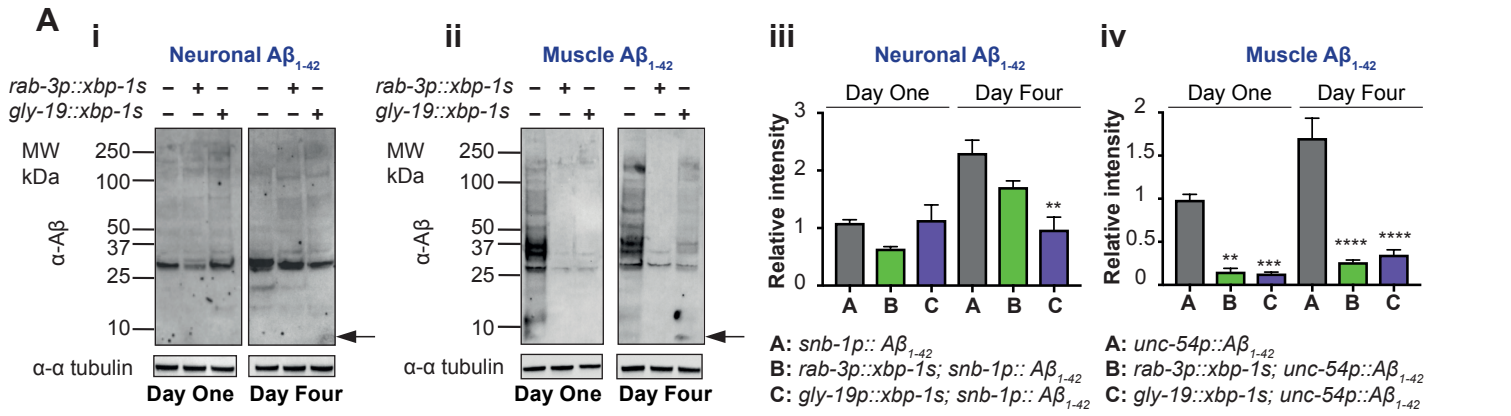


**Figure S1. Neuronal and intestinal *xbp-1s* reduce levels of toxic protein species. Related to Figure 2.**

(A) Reducing Western blot analysis of (i) neuronal A $\beta_{1-42}$  and (ii) muscle A $\beta_{1-42}$  with and without neuronal and intestinal *xbp-1s*, at day 1 and day 4 of adulthood. Lysates were resolved under reducing conditions and blotted with an anti-A $\beta$  antibody; the predicted MW of monomeric A $\beta_{1-42}$  is ~4.5 kDa, indicated with an arrow. Tubulin levels were probed with  $\alpha$ - $\alpha$  tubulin as a loading control. Blots were quantified using ImageJ (iii-iv). Graphs represent mean lane intensity relative to day 1 A $\beta_{1-42}$   $\pm$  SD and statistical significance was calculated between A and B/C at each time point using two-way ANOVA with Tukey's multiple comparisons test, \*\* $p < 0.01$ , \*\*\* $p < 0.001$ , \*\*\*\* $p < 0.0001$ . Data are representative of 3 independent experiments.

(B) Native Western blot analysis of (i) neuronal polyQ<sub>40</sub>::YFP, (ii) intestinal polyQ<sub>40</sub>::YFP and (iii) muscle polyQ<sub>35</sub>::YFP with and without tissue-specific *xbp-1s*, at day 1 and day 4 of adulthood. Lysates were resolved under native conditions and blotted with an anti-YFP/GFP antibody. The predicted MW of monomeric polyQ<sub>35-40</sub>:YFP is ~32 kDa – HMW indicates the higher molecular weight, polyQ-reactive band, while lower molecular weight, non-polyQ-reactive bands are likely to represent YFP cleaved from polyQ. Tubulin levels were probed with  $\alpha$ - $\alpha$  tubulin as a loading control. Data are representative of at least 2 independent experiments. Blots were quantified using ImageJ (iv-vi). Bar graphs represent mean band intensity relative to day 1 polyQ  $\pm$  standard deviation (SD) and statistical significance was calculated between A and B/C at each time point using two-way ANOVA with Tukey's multiple comparisons test, \* $p < 0.05$ , \*\* $p < 0.01$ , \*\*\* $p < 0.001$ , \*\*\*\* $p < 0.0001$ .

(C) Reducing Western blot analysis of (i) neuronal polyQ<sub>40</sub>::YFP, (ii) intestinal polyQ<sub>40</sub>::YFP and (iii) muscle polyQ<sub>35</sub>::YFP expressed with and without tissue-specific *xbp-1s*, at day 1 and day 4 of adulthood. Lysates were resolved under reducing conditions and blotted with an anti-polyQ antibody; the predicted MW of monomeric polyQ<sub>35-40</sub>::YFP is ~32 kDa. Tubulin levels were probed with  $\alpha$ - $\alpha$  tubulin as a loading control. Blots were quantified using ImageJ (iv-vi). Bar graphs represent mean band intensity relative to day 1 polyQ  $\pm$  SD and statistical significance was calculated between A and B/C at each time point using a two-way ANOVA with Tukey's multiple comparisons test, \* $p < 0.05$ , \*\* $p < 0.01$ , \*\*\* $p < 0.001$ , \*\*\*\* $p < 0.0001$ . Data are representative of at least 3 independent experiments.

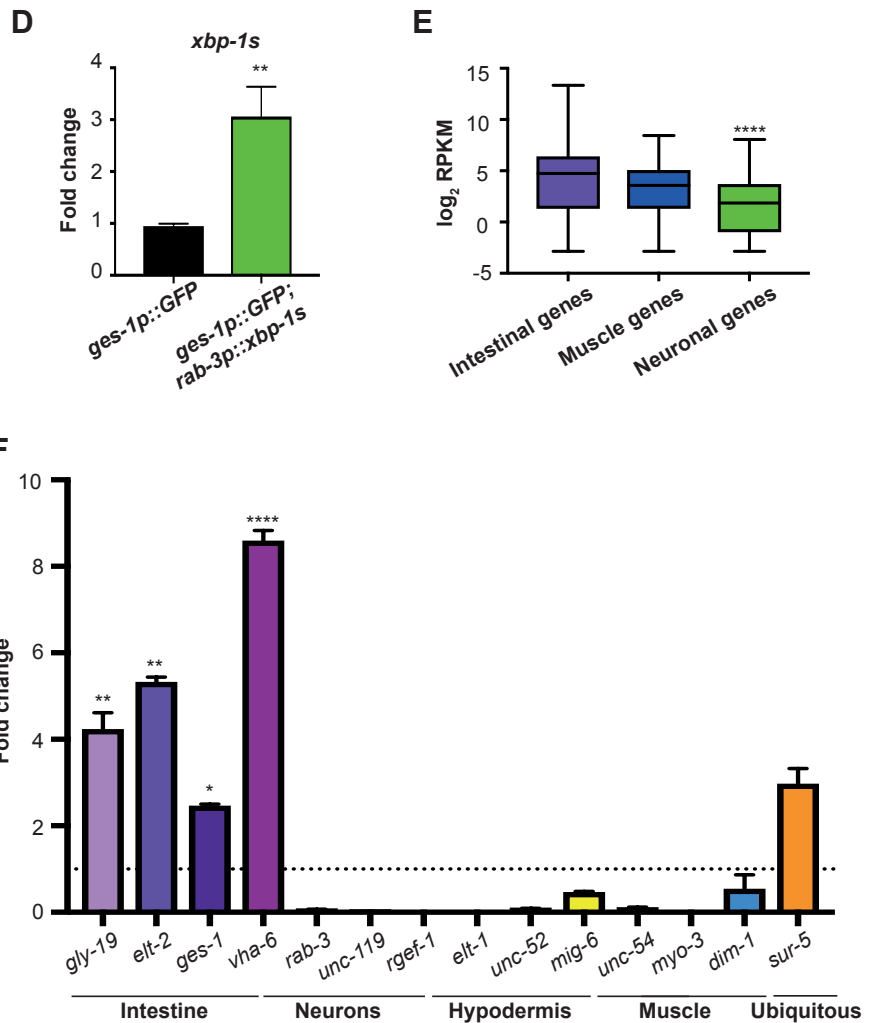
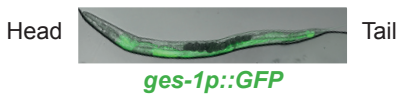
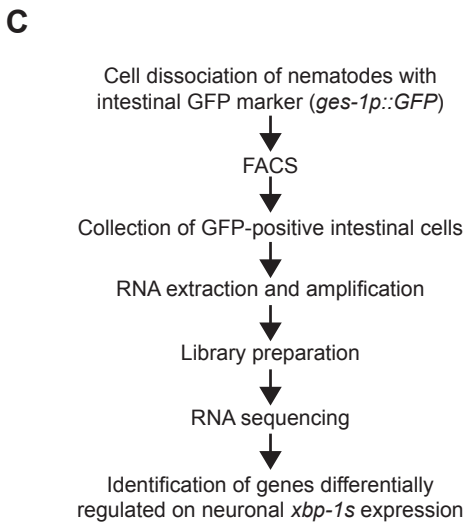
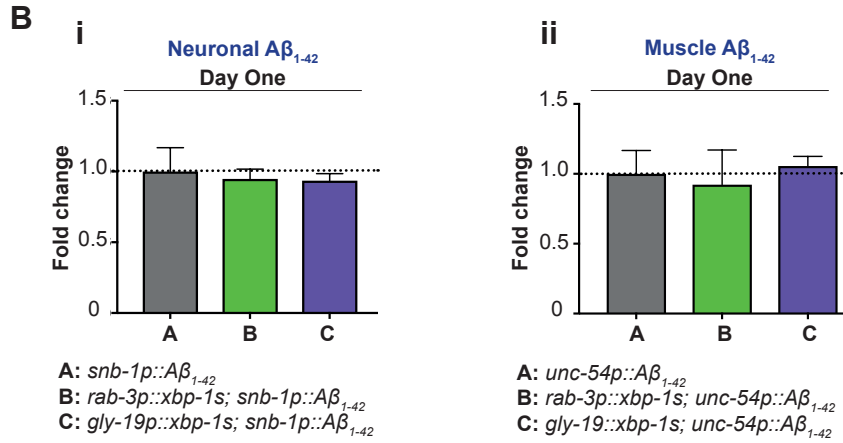
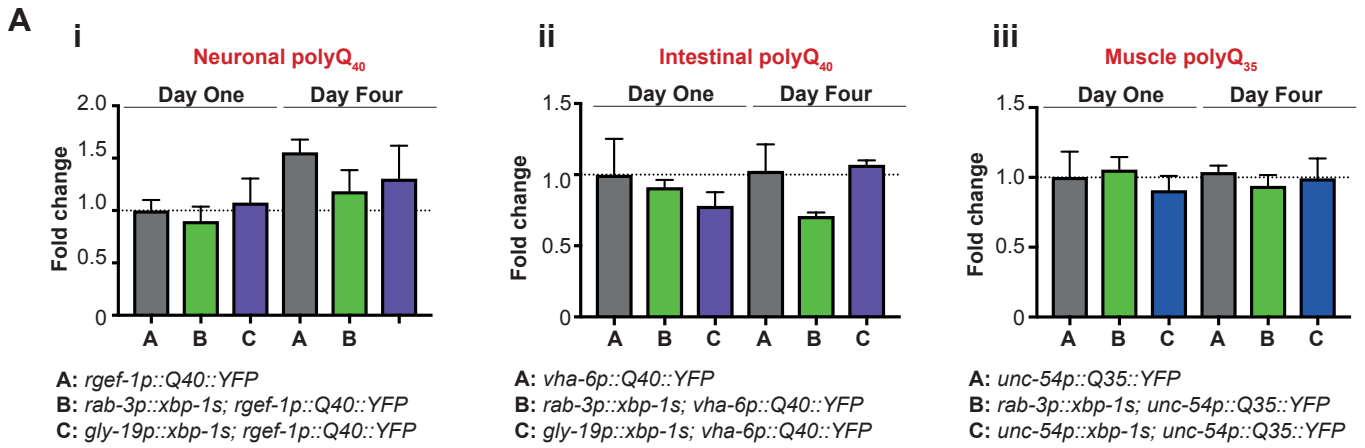


**Figure S2. Measurement of polyQ and A $\beta$ <sub>1-42</sub> transcript levels and validation of intestine-specific RNA-seq analysis. Related to Figures 2 and 3.**

(A) qPCR of YFP transcript levels in animals expressing (i) neuronal polyQ<sub>40</sub>::YFP, (ii) intestinal polyQ<sub>40</sub>::YFP and (iii) muscle polyQ<sub>35</sub>::YFP expressed with and without tissue-specific *xbp-1s*. YFP expression was measured at day 1 and day 4 of adulthood and normalized to day 1 polyQ alone. Significance was measured by one-way ANOVA with Tukey's multiple comparisons test.

(B) qPCR of A $\beta$ <sub>1-42</sub> transcript levels in animals expressing (i) neuronal A $\beta$ <sub>1-42</sub> and (ii) muscle A $\beta$ <sub>1-42</sub> with and without neuronal and intestinal *xbp-1s*. A $\beta$ <sub>1-42</sub> expression was measured at day 1 of adulthood and *xbp-1s*-expressing animals normalized to A $\beta$ <sub>1-42</sub> alone. Significance was measured by one-way ANOVA with Tukey's multiple comparisons test.

(C) Workflow of intestine-specific RNA-seq analysis. Cells from nematodes expressing the *ges-1p::GFP* intestinal marker are dissociated and collected using fluorescence-activated cell sorting (FACS). RNA is then extracted and amplified using the Ovation RNA-Seq System V2 before library preparation using the Ovation® Ultralow Library System. This RNA is sequenced and analyzed by intensity difference filtration to identify genes that are differentially regulated between *ges-1p::GFP* worms with and without neuronal *xbp-1s*. A confocal overlay micrograph of *ges-1p::GFP* worms is shown at X10 magnification.

(D) qPCR of *xbp-1s* transcript levels in intestinal cells of wild type and *rab-3p::xbp-1s*-expressing animals. Intestinal cells were isolated at day 1 of

adulthood from animals expressing *ges-1p::GFP* with and without *rab-3p::xbp-1s*, *xbp-1s* transcript levels measured, and *xbp-1*-expressing animals normalized to *ges-1p::GFP* alone. Significance was measured by one-way ANOVA with Tukey's multiple comparisons test, \*\* $p < 0.01$ .

(E) Box and whisker plots of intestinal, muscle and neuronal gene expression levels in the RNA-seq dataset. Tissue-specific genes were identified using the Princeton "Tissue-specific expression predictions for *C. elegans*" database (<http://worm-tissue.princeton.edu/search/download>) and the distribution of expression levels of these genes in RNA-seq samples plotted. Significance between intestine-specific and muscle- or neuron-specific gene categories was measured by student's t-test, using expression of each tissue-specific gene as one sample, \*\*\*\* $p < 0.0001$ .

(F) Validation of intestinal enrichment by qRT-PCR analysis of tissue-specific transcripts. Levels of 4 intestinal transcripts - *gly-19*, *elt-2*, *ges-1*, *vha-6*; 3 neuronal transcripts - *rab-3*, *unc-119*, *rgef-1*; 3 hypodermal transcripts - *elt-1*, *unc-52*, *mig-6*; 3 muscle transcripts - *unc-54*, *myo-3*, *dim-1*; and 1 ubiquitous transcript - *sur-5*; were measured by qRT-PCR in RNA extracted from *ges-1p::GFP*-expressing isolated intestinal cells, and in RNA extracted from non-intestinal GFP-negative cells. Graphs represent mean transcript levels in sorted intestinal cells normalized to levels of each transcript in GFP-negative cells, from 3 independent biological replicates. Error bars represent standard error of the mean (SEM). Significance of enrichment was assessed by one-way ANOVA with Tukey's multiple comparisons test, \* $p < 0.05$ , \*\* $p < 0.001$ , \*\*\*\* $p < 0.0001$ .

**A**

Upregulated lysosomal gene	XBP-1s promoter binding sites (5'--3')	HLH-30 promoter binding sites (5'--3')
<i>asp-3</i>	ACGT core (-86 to -80)	-
<i>cpr-1</i>	ETS domain (-316 to -311; -88 to -83); ACGT core (-1975 to -1969; -730 to -724); UPRE B element (-1979 to -1969)	CLEAR domain (-152 to -147)
<i>cpr-2</i>	CCACG box (-827 to -822); ACGT core (-702 to -696)	-
<i>cpr-4</i>	ETS domain (-1859 to -1854); CCACG box (-1013 to -1008); ACGT core (-1042 to -1036; -459 to -453)	-
<i>cpr-5</i>	-	-
<i>imp-2</i>	CAAT box (-341 to -336)	CLEAR domain (-311 to -306)
<i>F57F5.1</i>	ACGT core (-373 to -367; -370 to -364)	CLEAR domain (-53 to -48)
<i>aagr-3</i>	CAAT box (+28 to +33); ACGT core (-427 to -421)	-
<i>asah-1</i>	CCACG box (-274 to -269; -82 to -77); ACGT core (-82 to -76)	CLEAR domain (-80 to -75)
<i>gba-2</i>	CAAT box (-802 to -797); ETS domain (-507 to -502)	-
<i>hex-1</i>	CAAT box (-353 to -348; -212 to -207); CCACG box (-1494 to -1489)	-
<i>lipl-1</i>	CCACG box (-985 to -980)	CLEAR domain (-444 to -439)
<i>lipl-5</i>	ACGT core (-1091 to -1085)	CLEAR domain (-51 to -46)
<i>spp-10</i>	-	CLEAR domain (-847 to -842)
<i>nuc-1</i>	ETS domain (-1617 to -1612); ACGT core (-295 to -289)	-
<i>cdr-1</i>	-	-
<i>lys-4</i>	-	CLEAR domain (-838 to -833)
<i>lys-8</i>	-	-
<i>ctns-1</i>	ETS domain (-1559 to -1554; -1827 to -1822)	-
<i>vha-18</i>	-	-
<i>blos-8</i>	CAAT box (-1430 to -1425)	-

Binding sites
CAAT box (5' -CCAATC- 3')
ETS domain (5' -CGGAAG- 3')
CCACG box (5' -GCCACG- 3')
ACGT core (5' -G(C/T)(C/G)ACGT- 3')
UPRE A element (5' -CGACGTGG- 3')
UPRE B element (5' -GTGACGTG- 3')
CLEAR domain (5' -CACGTG- 3')

**B**

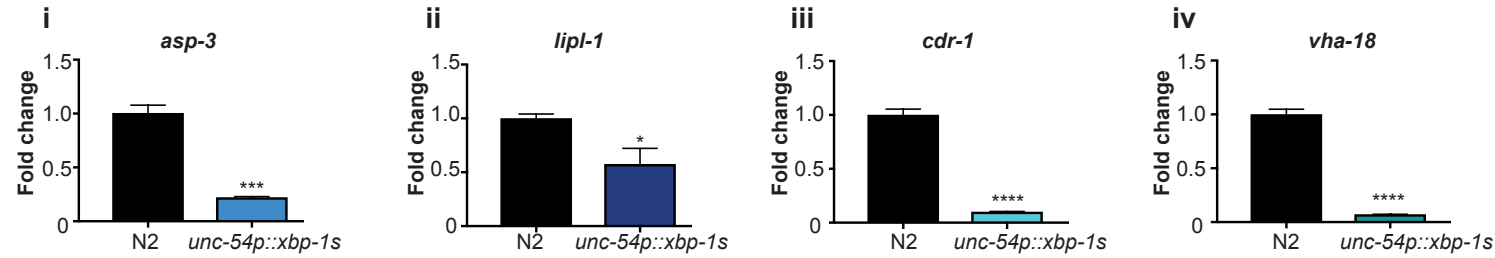
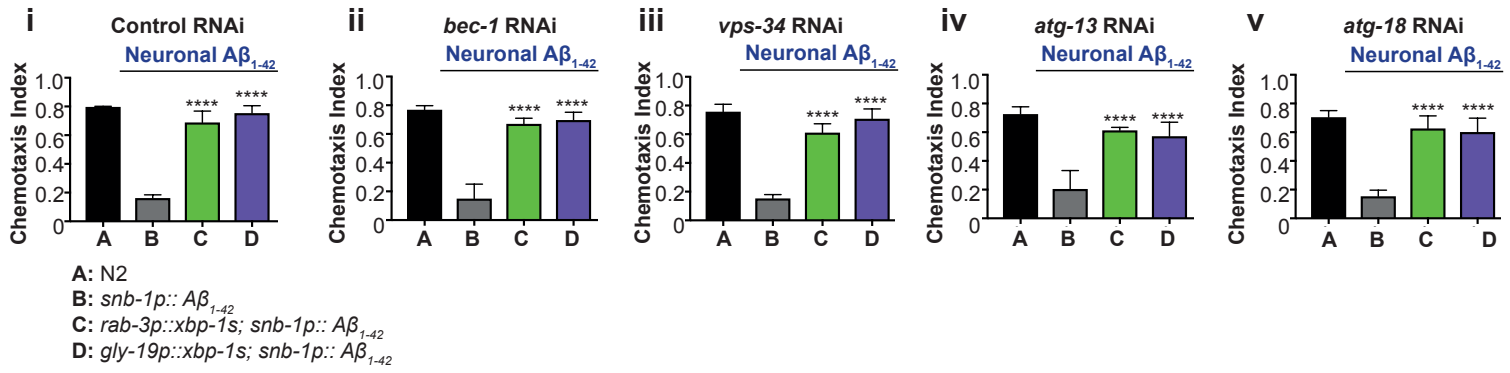


**Figure S3. Lysosomal genes may be direct and tissue-specific targets of *xbp-1s*. Related to Figure 3.**

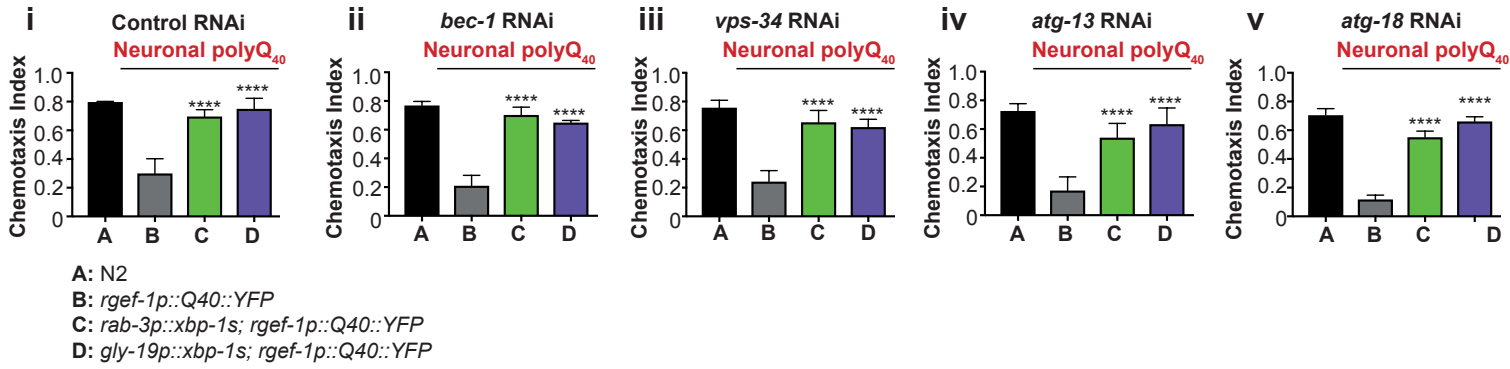
(A) *xbp-1s* and *hlh-30* binding sites in the promoters of lysosomal genes upregulated in the intestines of neuronal *xbp-1s*-expressing animals. Sites listed in the legend were searched for within promoter sequences as defined by the Harvard Promoterome Database.

(B) qRT-PCR of lysosomal gene transcript levels in all-tissue lysates from animals expressing *xbp-1s* in muscle cells relative to N2 nematodes: (i) *asp-3*, (ii) *lip1-1*, (iii) *cdr-1*, (iv) *vha-18*. Transcript levels were measured at day 1 of adulthood and *xbp-1*-expressing animals normalized to N2. Significance was measured by one-way ANOVA with Tukey's multiple comparisons test, \* $p < 0.05$ , \*\*\* $p < 0.001$ , \*\*\*\* $p < 0.0001$ .

**A**



**B**



**C**

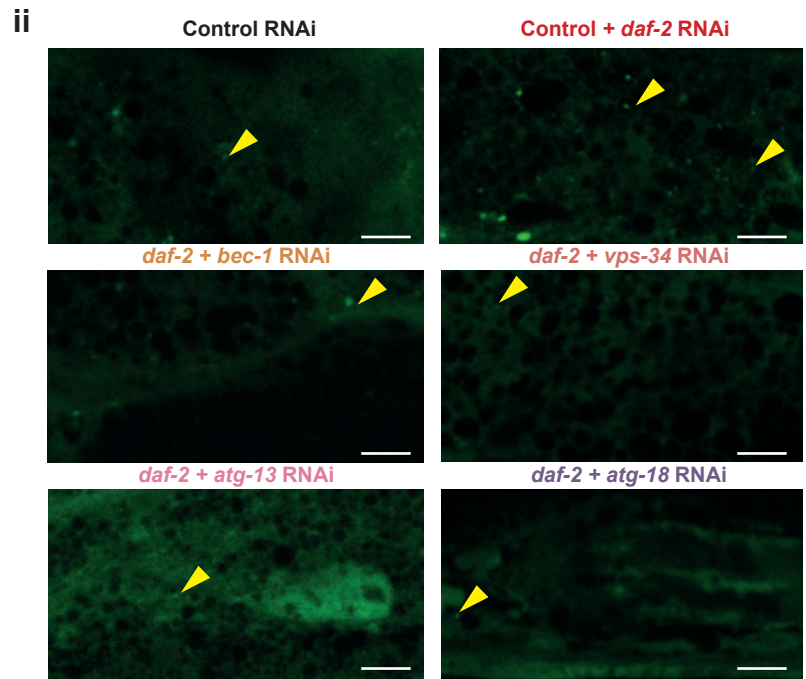
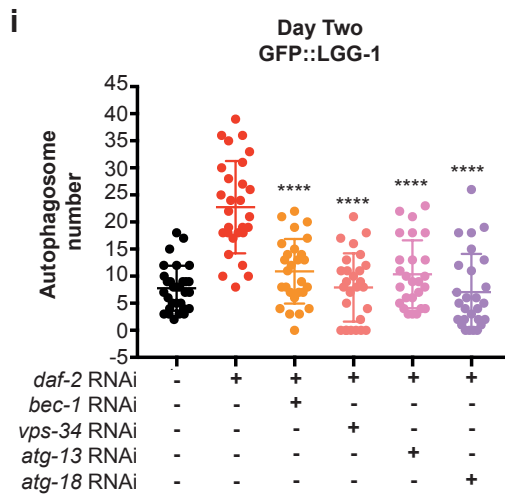


**Figure S4. Protection from proteotoxicity in *xbp-1s*-expressing animals does not depend upon genes involved in autophagy. Related to Figure 4.**

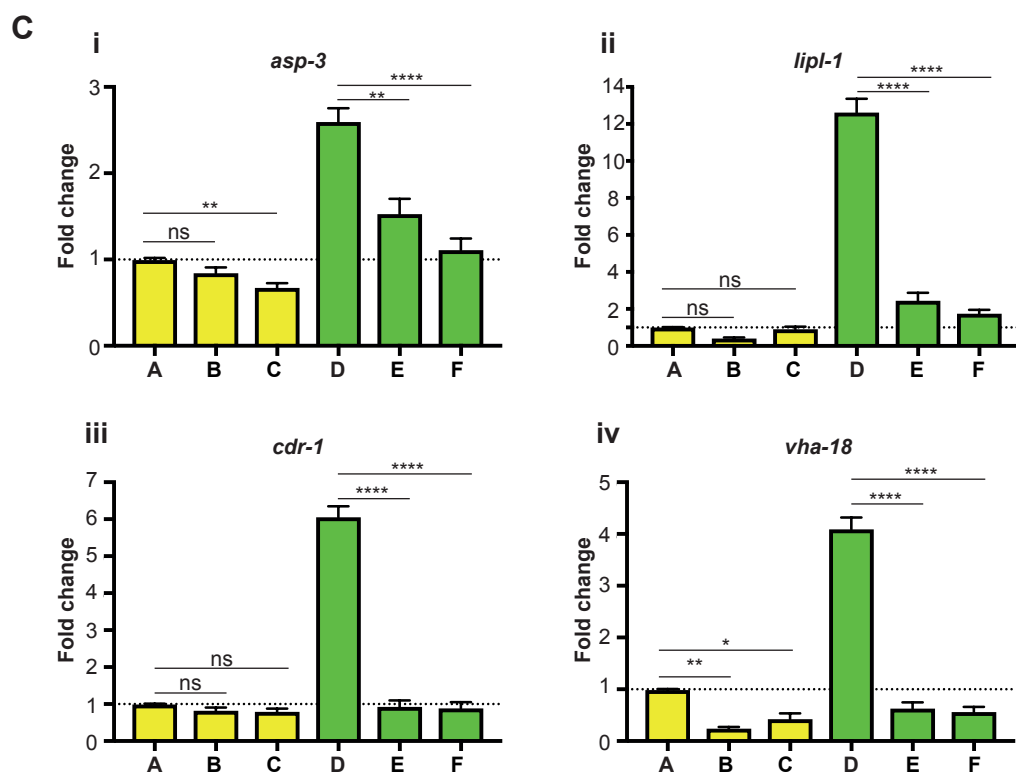
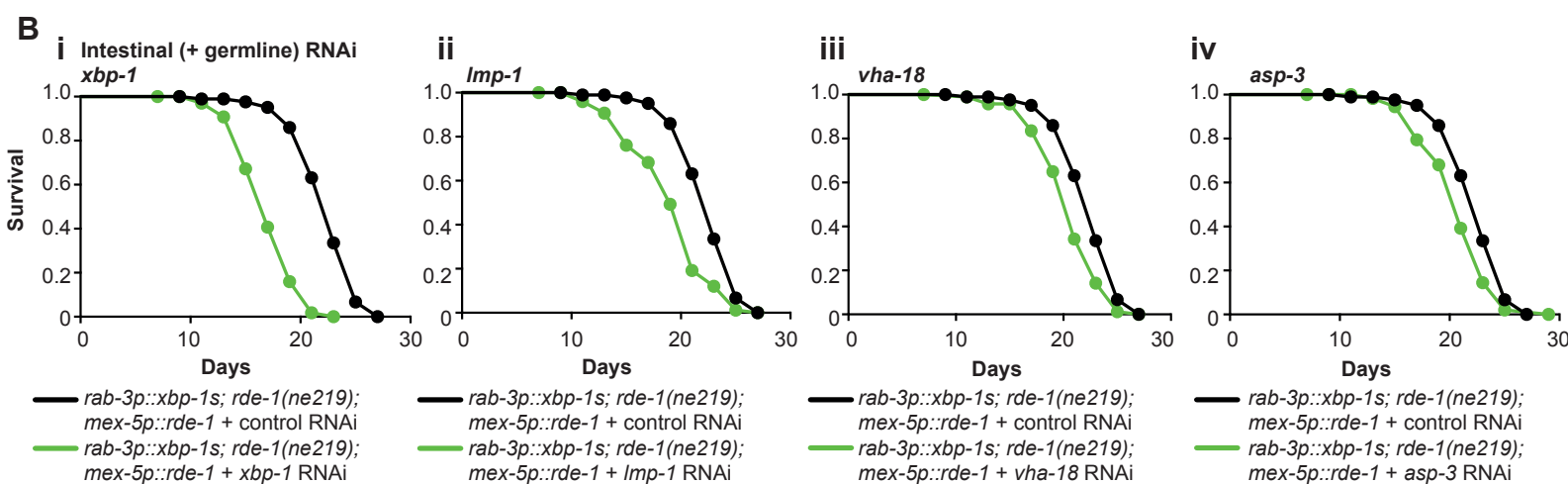
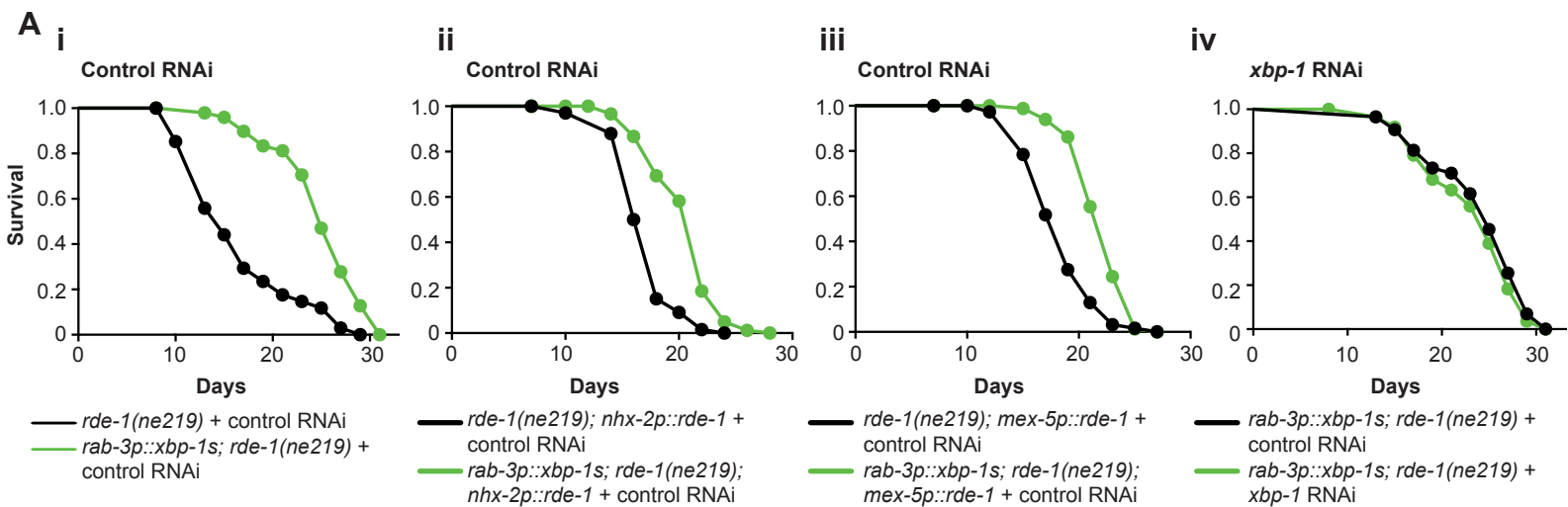
(A) Chemotaxis ability in animals expressing A $\beta$ <sub>1-42</sub> in neurons in combination with neuronal and intestinal *xbp-1s*, grown on (i) control (empty vector), (ii) *bec-1*, (iii) *vps-34*, (iv) *atg-13*, or (v) *atg-18* RNAi. Graphs represent mean chemotaxis index  $\pm$  SD. N = 80-150 animals per assay, and each assay was independently replicated 3 times. Significance between neuronal A $\beta$ <sub>1-42</sub> (B) and *xbp-1s*-expressing (C/D) strains was assessed by two-way ANOVA with Dunnett's multiple comparisons test, \*\*\*\*p<0.0001.

(B) Chemotaxis ability in animals expressing polyQ<sub>40</sub> in neurons in combination with neuronal and intestinal *xbp-1s*, grown on (i) control (empty vector), (ii) *bec-1*, (iii) *vps-34*, (iv) *atg-13*, or (v) *atg-18* RNAi. Graphs represent mean chemotaxis index  $\pm$  SD. N = 80-170 animals per assay, and each assay was independently replicated 3 times. Significance between neuronal polyQ<sub>40</sub> (B) and *xbp-1s*-expressing (C/D) strains was assessed by two-way ANOVA with Dunnett's multiple comparisons test, \*\*\*\*p<0.0001.

(C) (i) Quantification of autophagic vesicles. Animals were grown on control, control + *daf-2*, *daf-2* + *bec-1*, *daf-2* + *vps-34*, *daf-2* + *atg-13*, or *daf-2* + *atg-18* RNAi. GFP::LGG-1-positive punctae were imaged at X63 magnification and counted in 25-30 worms per genotype at day 2 of adulthood using ImageJ. Data are derived from 3 independent biological replicates. Statistical analysis was performed relative to control + *daf-2* RNAi, using one-way ANOVA with Tukey's multiple comparisons test, \*\*\*\*p<0.0001.

(ii) Representative confocal images of the intestine of animals expressing GFP::LGG-1, grown on control, control + *daf-2*, *daf-2* + *bec-1*, *daf-2* + *vps-34*,

*daf-2 + atg-13*, or *daf-2 + atg-18* RNAi. Animals were imaged at day 2 of adulthood, at X63 magnification. Scale bar = 5  $\mu$ m.



A: *rde-1(ne219); nhx-2p::rde-1* + control RNAi  
 B: *rde-1(ne219); nhx-2p::rde-1* + *xbp-1* RNAi  
 C: *rde-1(ne219); nhx-2p::rde-1* + *hlh-30* RNAi  
 D: *rab-3p::xbp-1s; rde-1(ne219); nhx-2p::rde-1* + control RNAi  
 E: *rab-3p::xbp-1s; rde-1(ne219); nhx-2p::rde-1* + *xbp-1* RNAi  
 F: *rab-3p::xbp-1s; rde-1(ne219); nhx-2p::rde-1* + *hlh-30* RNAi

**Figure S5. Validation of intestine-specific RNAi. Related to Figure 5 and Table S1.**

(A) (i) Lifespan analysis of *rde(n219)* and *rab-3p::xbp-1s; rde(n219)* animals grown on control (empty vector) RNAi. *rde(n219)*, control (black), median lifespan 15 days; *rab-3p::xbp-1s; rde(n219)*, control (green), median lifespan 25 days,  $p < 0.0001$ . Graph plotted as a Kaplan-Meier survival curve, P value calculated by Mantel-Cox log-rank test; N = 80-120 animals per lifespan.

(ii) Lifespan analysis of *rde(n219); nhx-2p::rde-1* and *rab-3p::xbp-1s; rde(n219); nhx-2p::rde-1* animals grown on control (empty vector) RNAi. *rde(n219); nhx-2p::rde-1*, control (black), median lifespan 18 days; *rab-3p::xbp-1s; rde(n219); nhx-2p::rde-1*, control (green), median lifespan 22 days,  $p < 0.0001$ . Graph plotted as a Kaplan-Meier survival curve, P value calculated by Mantel-Cox log-rank test; N = 80-120 animals per lifespan.

(iii) Lifespan analysis of *rde(n219); mex-5p::rde-1* and *rab-3p::xbp-1s; rde(n219); mex-5p::rde-1* animals grown on control (empty vector) RNAi. *rde(n219); mex-5p::rde-1*, control (black), median lifespan 19 days; *rab-3p::xbp-1s; rde(n219); mex-5p::rde-1*, control (green), median lifespan 23 days,  $p < 0.0001$ . Graph plotted as a Kaplan-Meier survival curve, P value calculated by Mantel-Cox log-rank test; N = 80-120 animals per lifespan.

(iv) Lifespan analysis of *rab-3p::xbp-1s; rde(n219)* animals grown on control (empty vector) and *xbp-1* RNAi. *rab-3p::xbp-1s; rde(n219)*, control (black), median lifespan 25 days; *rab-3p::xbp-1s; rde(n219), xbp-1* (green), median lifespan 25 days,  $p = 0.2281$ . Graph plotted as a Kaplan-Meier survival curve, P value calculated by Mantel-Cox log-rank test; N = 80-120 animals per lifespan.

(B) Lifespan analysis of *rab-3p::xbp-1s; rde(n219); mex-5p::rde-1* animals grown on control (empty vector) or (i) *xbp-1*, (ii) *Imp-1*, (iii) *vha-18*, or (iv) *asp-3* RNAi. Graphs were plotted as Kaplan-Meier survival curves, P values were calculated by Mantel-Cox log-rank test.

(i) *rab-3p::xbp-1s; rde(n219); mex-5p::rde-1*, control (black), median lifespan 23 days; *rab-3p::xbp-1s; rde(n219); mex-5p::rde-1, xbp-1* (green), median lifespan 17 days,  $p < 0.0001$ .

(ii) *rab-3p::xbp-1s; rde(n219); mex-5p::rde-1*, control (black), median lifespan 23 days; *rab-3p::xbp-1s; rde(n219); mex-5p::rde-1, Imp-1* (green), median lifespan 19 days,  $p < 0.0001$ .

(iii) *rab-3p::xbp-1s; rde(n219); mex-5p::rde-1*, control (black), median lifespan 23 days; *rab-3p::xbp-1s; rde(n219); mex-5p::rde-1, vha-18* (green), median lifespan 21 days,  $p < 0.0001$ .

(iv) *rab-3p::xbp-1s; rde(n219); mex-5p::rde-1*, control (black), median lifespan 23 days; *rab-3p::xbp-1s; rde(n219); mex-5p::rde-1, asp-3* (green), median lifespan 21 days,  $p < 0.01$ .

(C) qPCR of (i) *asp-3*, (ii) *lip1-1*, (iii) *cdr-1* and (iv) *vha-18* transcript levels at day 1 of adulthood in *rde-1(ne219); nhx-2p::rde-1* animals, with and without *rab-3p::xbp-1s* expression, grown on control, *xbp-1* or *hlh-30* RNAi. Expression was normalized to *rde-1(ne219); nhx-2p::rde-1* on control RNAi and significance measured by one-way ANOVA with Tukey's multiple comparisons test, ns = not significant, \* $p < 0.05$ , \*\* $p < 0.01$ , \*\*\*\* $p < 0.0001$ .

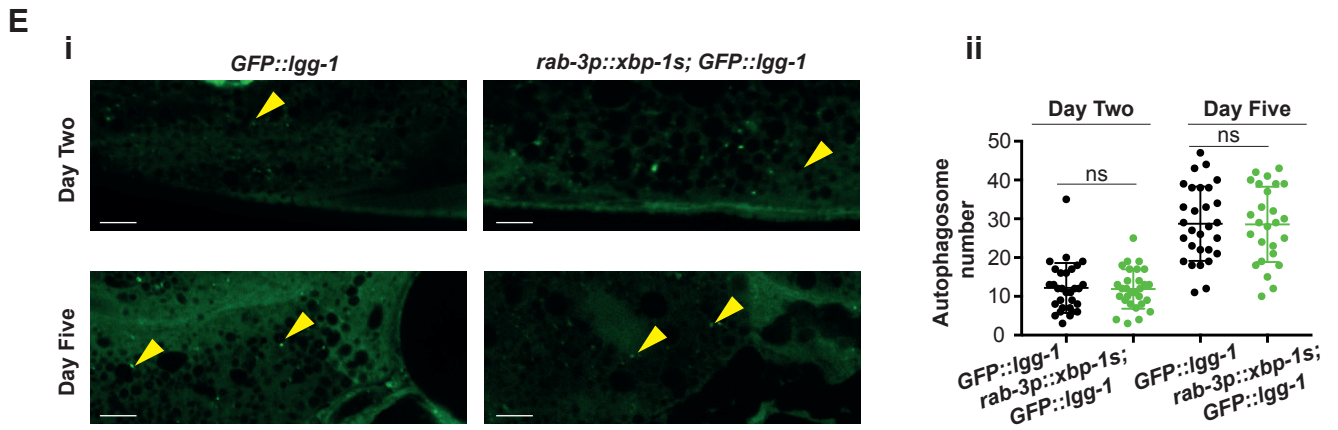
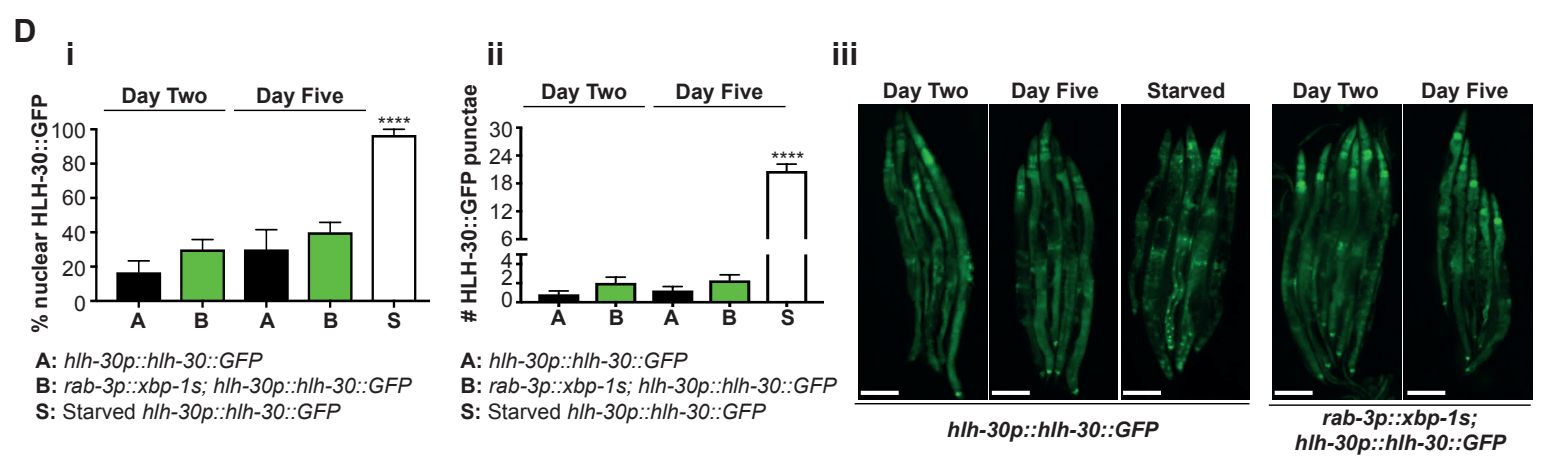
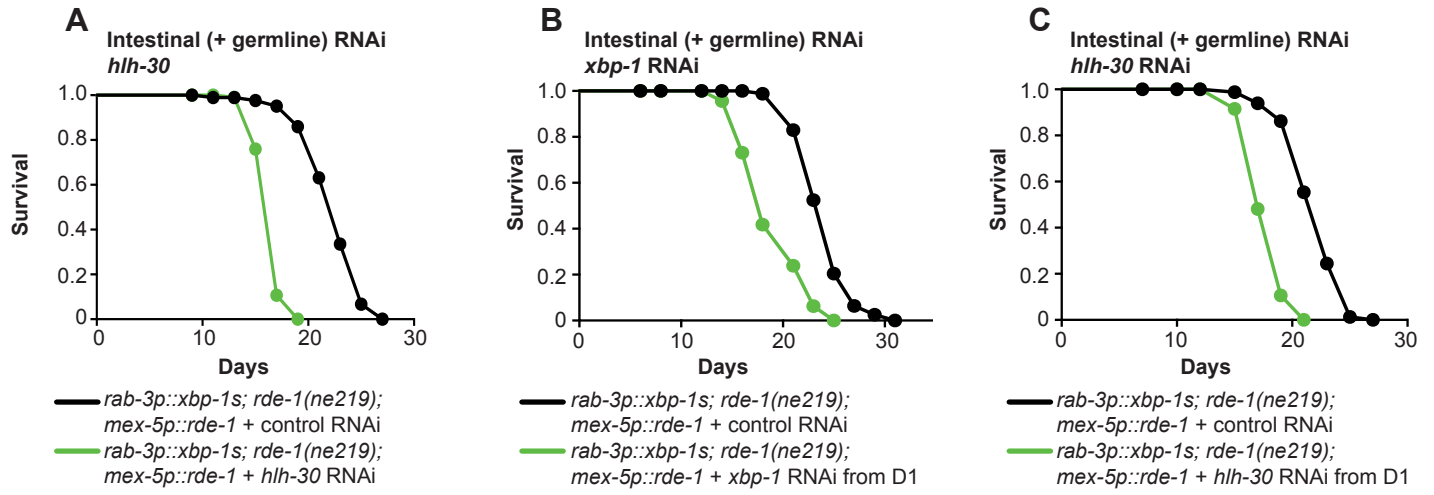


**Figure S6. Analysis of HLH-30 and LGG-1 localization in intestinal cells.  
Related to Figures 5 and 6 and Table S1.**

(A) Lifespan analysis of *rab-3p::xbp-1s; rde(n219); mex-5p::rde-1* animals grown on control (empty vector) or *hlh-30* RNAi. *rab-3p::xbp-1s; rde(n219); mex-5p::rde-1*, control (black), median lifespan 23 days; *rab-3p::xbp-1s; rde(n219); mex-5p::rde-1, hlh-30* (green), median lifespan 17 days,  $p < 0.0001$ . Graphs were plotted as Kaplan-Meier survival curves, P values were calculated by Mantel-Cox log-rank test.

(B) Lifespan analysis of *rab-3p::xbp-1s; rde(n219); mex-5p::rde-1* animals grown on control (empty vector) RNAi throughout life, or on control (empty vector) RNAi until day 1 of adulthood and transferred to *xbp-1* RNAi from this age. *rab-3p::xbp-1s; rde(n219); mex-5p::rde-1*, control (black), median lifespan 25 days; *rab-3p::xbp-1s; rde(n219); mex-5p::rde-1, xbp-1* from adulthood (green), median lifespan 18 days,  $p < 0.0001$ . Graph plotted as a Kaplan-Meier survival curve, P value calculated by Mantel-Cox log-rank test; N = 80-120 animals per lifespan.

(C) Lifespan analysis of *rab-3p::xbp-1s; rde(n219); mex-5p::rde-1* animals grown on control (empty vector) RNAi throughout life, or on control (empty vector) RNAi until day 1 of adulthood and transferred to *hlh-30* RNAi from this age. *rab-3p::xbp-1s; rde(n219); mex-5p::rde-1*, control (black), median lifespan 23 days; *rab-3p::xbp-1s; rde(n219); mex-5p::rde-1, hlh-30* from adulthood (green), median lifespan 17 days,  $p < 0.0001$ . Graph plotted as a Kaplan-Meier survival curve, P value calculated by Mantel-Cox log-rank test; N = 80-120 animals per lifespan.

(D) (i) Quantification of HLH-30::GFP nuclear localization. Numbers of animals with nuclear HLH-30::GFP in the intestine were quantified at day 2 and day 5 of adulthood (except starved animals which were quantified at day 2 only); graphs represent mean percentage of animals with nuclear HLH-30::GFP  $\pm$  SEM. N = 30 animals per assay, independently replicated 3 times. Significance was assessed by one-way ANOVA with Tukey's multiple comparisons test, \*\*\*\* $p < 0.0001$ .

(ii) Quantification of HLH-30::GFP-positive nuclei per animal. Numbers of HLH-30::GFP-positive nuclei in the intestine were quantified per animal at day 2 and day 5 of adulthood (except starved animals which were quantified at day 2 only); graphs represent mean percentage of animals with nuclear HLH-30::GFP  $\pm$  SEM. N = 30 animals per assay, independently replicated 3 times. Significance was assessed by one way ANOVA with Tukey's multiple comparisons test, \*\*\*\* $p < 0.0001$ .

(iii) Confocal images of animals expressing HLH-30::GFP with and without *rab-3p::xbp-1s* at day 2 and day 5 of adulthood, alongside starved animals expressing HLH-30::GFP at day 2. Scale bar = 100  $\mu\text{m}$ .

(E) (i) Representative confocal images of the intestine of animals expressing GFP::LGG-1, with and without *rab-3p::xbp-1s*. Animals were grown on OP50 and imaged at days 2 and 5 of adulthood. Imaging was performed at X63 magnification. Arrowheads indicate representative autophagosomes. Scale bar = 5  $\mu\text{m}$ .

(ii) Quantification of autophagic vesicles. GFP::LGG-1-positive punctae were imaged at X63 magnification and counted in 10-15 worms per genotype at day 2 and day 5 of adulthood using ImageJ. Data are derived from 3

independent biological replicates. Statistical analysis was performed using one-way ANOVA with Tukey's multiple comparisons test. ns = not significant.

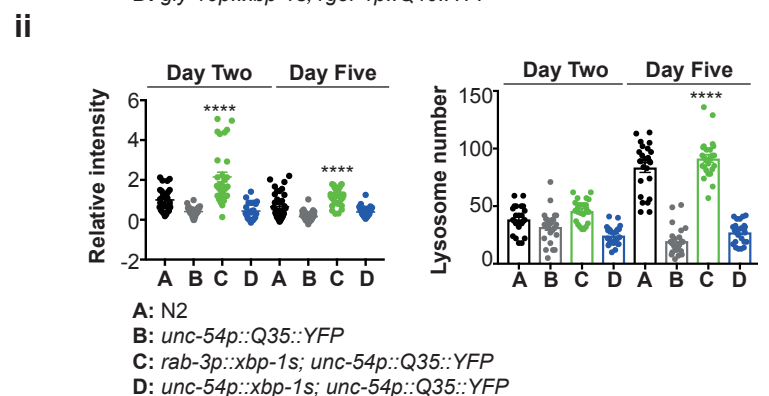
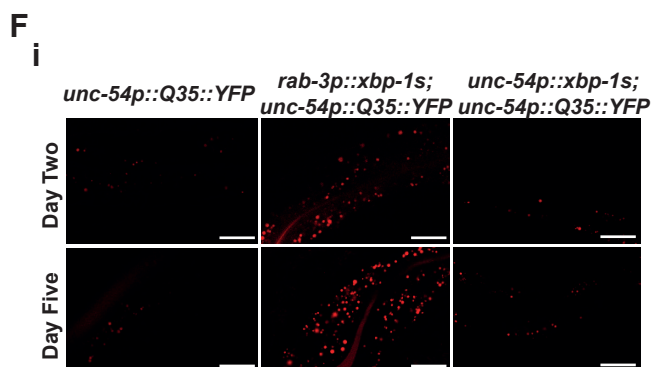
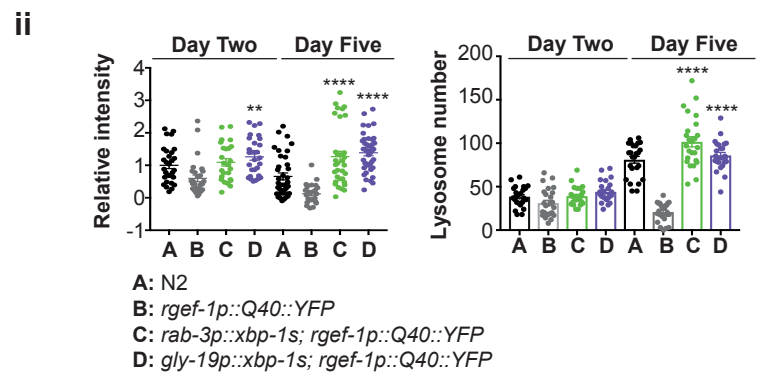
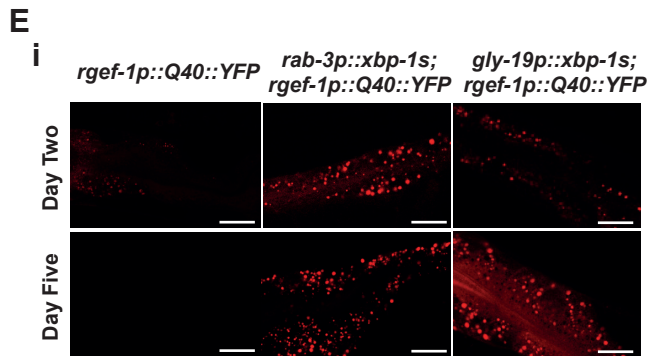
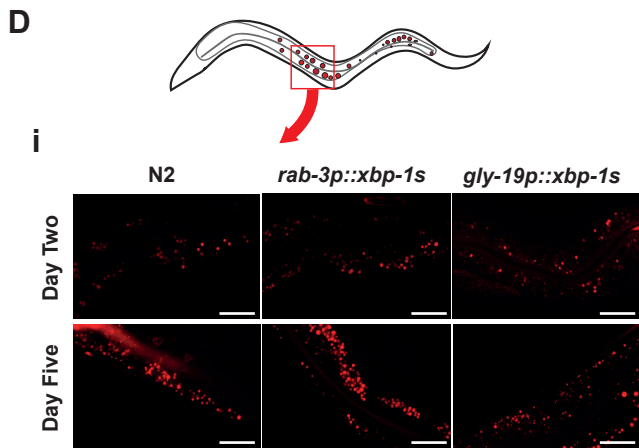
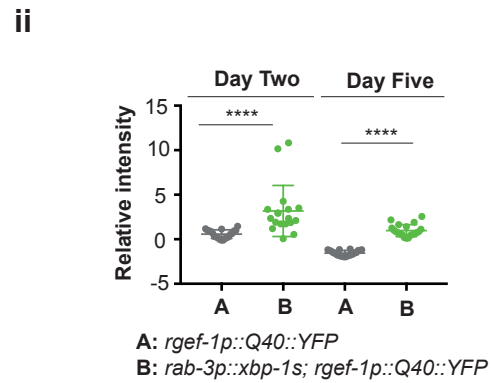
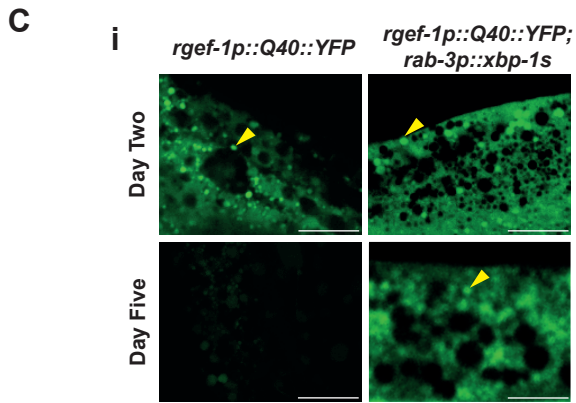
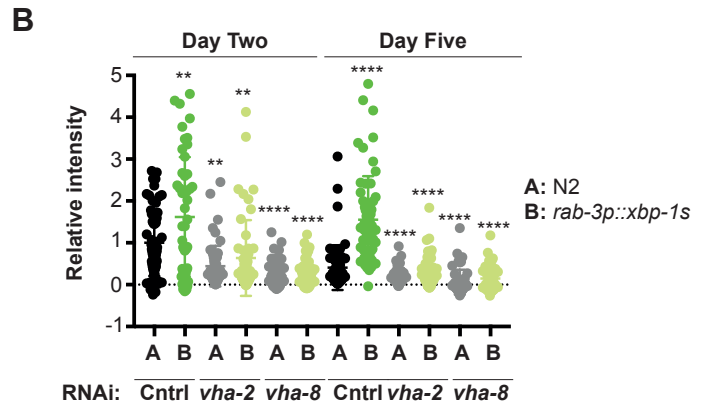
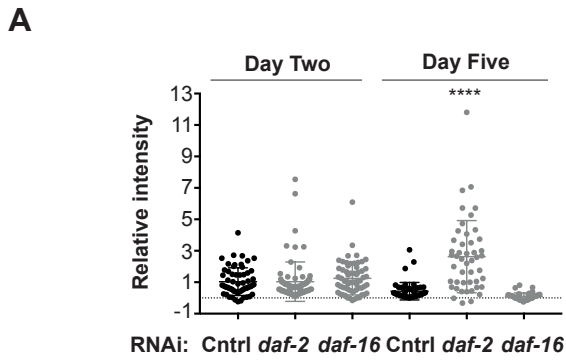


**Figure S7. Validation of lysosomal acidity staining and analysis of lysosomal acidity in animals expressing polyQ expansions. Related to Figure 7.**

(A) Quantification of lysosomal acidity in the intestine of animals grown on control (empty vector), *daf-2* or *daf-16* RNAi. Animals were transferred to plates containing cDCFDA 16 hours prior to imaging. Using X63 magnification, imaging was conducted at day 2 and day 5 of adulthood. Quantification of fluorescence from 3 experiments was carried out using ImageJ. Plots represent 10 animals per replicate. Significance was assessed at each time point by an ordinary one-way ANOVA with Tukey's multiple comparisons, \*\*\*\* $p < 0.0001$ .

(B) Quantification of lysosomal acidity in the intestine of N2 and *rab-3p::xbp-1s*-expressing animals grown on control, *vha-2* or *vha-8* RNAi. Animals were transferred to plates containing cDCFDA 16 hours prior to imaging. Using X63 magnification, imaging was conducted at day 2 and day 5 of adulthood. Quantification of fluorescence from 3 experiments was carried out using ImageJ. Plots represent 10 animals per replicate. Significance was assessed in each genotype relative to control RNAi at both time points by ordinary one-way ANOVA with Tukey's multiple comparisons, \*\* $p < 0.01$ , \*\*\*\* $p < 0.0001$ .

(C) (i) Confocal imaging of acidic lysosomes in the intestine of neuronal polyQ<sub>40</sub> animals, with and without neuronal *xbp-1s*. Animals were grown on OP50 and transferred to plates containing cDCFDA 16 hours prior to imaging. Using X63 magnification, imaging was conducted at day 2 and day 5 of adulthood. Scale bar = 10  $\mu\text{m}$ .

(ii) Quantification of lysosomal acidity in the intestine of neuronal polyQ<sub>40</sub> animals, with and without neuronal *xbp-1s*. Animals were grown on OP50 and transferred to plates containing cDCFDA 16 hours prior to imaging and imaged as (D); quantification of fluorescence from 2 experiments was carried out using ImageJ. Plots represent 5-10 animals per replicate. Significance was assessed between N2 and *rab-3p::xbp-1s* at each time point by one-way ANOVA with Tukey's multiple comparisons, \*\*\*\*p<0.0001.

(D) (i) Confocal imaging of N2, *rab-3p::xbp-1s* and *gly-19p::xbp-1s* nematodes stained with LysoTracker Deep Red at days 2 and 5 of adulthood. Scale bar = 20  $\mu$ m.

(ii) Quantification of intensity and number of LysoTracker-stained punctae in animals imaged as above. ImageJ was used to assess fluorescence intensity, which was normalized to N2. Each plot represents mean  $\pm$  SEM from 3 independent biological replicates, N = 8-10 animals per replicate. Significance was calculated using one way ANOVA with Tukey's multiple comparisons test, \*\*p<0.01, \*\*\*p<0.001, \*\*\*\*p<0.0001.

(E) (i) Confocal imaging of *rgef-1p::Q40::YFP* animals with or without *rab-3p::xbp-1s* and *gly-19p::xbp-1s*, stained with LysoTracker Deep Red at days 2 and 5 of adulthood. Scale bar = 20  $\mu$ m.

(ii) Quantification of intensity and number of LysoTracker-stained punctae in *rgef-1p::Q40::YFP* animals imaged as above. ImageJ was used to assess fluorescence intensity, which was normalized to N2. Each plot represents mean  $\pm$  SEM from 3 independent biological replicates, N = 8-10 animals per replicate. Significance was calculated using one way ANOVA with Tukey's multiple comparisons test, \*\*p<0.01, \*\*\*\*p<0.0001.

(F) (i) Confocal imaging of *unc-54p::Q35::YFP* animals with or without *rab-3p::xbp-1s* and *unc-54p::xbp-1s*, stained with LysoTracker Deep Red at days 2 and 5 of adulthood. Scale bar = 20  $\mu\text{m}$ .

(ii) Quantification of intensity and number of LysoTracker-stained punctae in *unc-54p::Q35::YFP* animals imaged as above. ImageJ was used to assess fluorescence intensity, which was normalized to N2. Each plot represents mean  $\pm$  SEM from 3 independent biological replicates, N = 8-10 animals per replicate. Significance was calculated using one way ANOVA with Tukey's multiple comparisons test, \*\*\*\* $p < 0.0001$ .